



*Citation for published version:*

Chung, J & Gazzola, S 2019, 'Flexible Krylov Methods for  $L_1$  regularization', *SIAM Journal on Scientific Computing*, vol. 41, no. 5, pp. S149-S171. <https://doi.org/10.1137/18M1194456>

*DOI:*

[10.1137/18M1194456](https://doi.org/10.1137/18M1194456)

*Publication date:*

2019

*Document Version*

Peer reviewed version

[Link to publication](#)

Copyright © 2019 Society for Industrial and Applied Mathematics. The final publication is available at SIAM Journal on Scientific Computing via <https://doi.org/10.1137/18M1194456>.

**University of Bath**

## **Alternative formats**

If you require this document in an alternative format, please contact:  
[openaccess@bath.ac.uk](mailto:openaccess@bath.ac.uk)

### **General rights**

Copyright and moral rights for the publications made accessible in the public portal are retained by the authors and/or other copyright owners and it is a condition of accessing publications that users recognise and abide by the legal requirements associated with these rights.

### **Take down policy**

If you believe that this document breaches copyright please contact us providing details, and we will remove access to the work immediately and investigate your claim.

# 1 FLEXIBLE KRYLOV METHODS FOR $\ell_p$ REGULARIZATION\*

2 JULIANNE CHUNG<sup>†</sup> AND SILVIA GAZZOLA<sup>‡</sup>

3 **Abstract.** In this paper we develop flexible Krylov methods for efficiently computing regularized  
 4 solutions to large-scale linear inverse problems with an  $\ell_2$  fit-to-data term and an  $\ell_p$  penalization  
 5 term, for  $p \geq 1$ . First we approximate the  $p$ -norm penalization term as a sequence of 2-norm penaliza-  
 6 tion terms using adaptive regularization matrices in an iterative reweighted norm fashion, and then  
 7 we exploit flexible preconditioning techniques to efficiently incorporate the weight updates. To han-  
 8 dle general (non-square)  $\ell_p$ -regularized least-squares problems, we introduce a flexible Golub–Kahan  
 9 approach and exploit it within a Krylov–Tikhonov hybrid framework. Furthermore, we show that  
 10 both the flexible Golub–Kahan and the flexible Arnoldi approaches for  $p = 1$  can be used to efficiently  
 11 compute solutions that are sparse with respect to some transformations. The key benefits of our ap-  
 12 proach compared to existing optimization methods for  $\ell_p$  regularization are that inner-outer iteration  
 13 schemes are replaced by efficient projection methods on linear subspaces of increasing dimension and  
 14 that expensive regularization parameter selection techniques can be avoided. Theoretical insights  
 15 are provided, and numerical results from image deblurring and tomographic reconstruction illustrate  
 16 the benefits of this approach, compared to well-established methods.

17 **Keywords:**  $\ell_p$  regularization, sparsity reconstruction, iterative reweighted norm,  
 18 flexible Golub–Kahan, hybrid regularization, image deblurring, tomographic recon-  
 19 struction.

20 **1. Introduction.** Inverse problems are prevalent in many important applica-  
 21 tions, ranging from biomedical to geophysical imaging, and solutions must be com-  
 22 puted reliably and efficiently. In this work we consider discretized linear inverse  
 23 problems of the form

$$24 \quad (1) \quad \mathbf{b} = \mathbf{A}\mathbf{x}_{\text{true}} + \mathbf{e},$$

25 where  $\mathbf{b} \in \mathbb{R}^m$  is the observed data,  $\mathbf{A} \in \mathbb{R}^{m \times n}$  is the ill-conditioned matrix that  
 26 models the forward process,  $\mathbf{x}_{\text{true}} \in \mathbb{R}^n$  is the desired solution, and  $\mathbf{e} \in \mathbb{R}^m$  is the  
 27 noise or perturbation affecting the observation. Due to the ill-posedness of the under-  
 28 lying problem, in order to recover a meaningful approximation of  $\mathbf{x}_{\text{true}}$  in (1), some  
 29 regularization is applied, i.e., problem (1) is replaced by a closely related one that  
 30 is stable with respect to the corrupted data [18]. In this paper, we are interested in  
 31 regularized problems of the form

$$32 \quad (2) \quad \min_{\mathbf{x}} \|\mathbf{A}\mathbf{x} - \mathbf{b}\|_2^2 + \lambda \|\Psi\mathbf{x}\|_p^p,$$

33 where  $\|\cdot\|_p$  for  $p \geq 1$  is the vectorial  $p$ -norm,  $\lambda > 0$  is a regularization parameter,  
 34 and  $\Psi \in \mathbb{R}^{n \times n}$  is a nonsingular matrix. For  $p = 2$  and  $\Psi = \mathbf{I}$ , (2) is the standard  
 35 Tikhonov regularization problem, and many efficient techniques including hybrid iter-  
 36 ative methods have been proposed, see, e.g., [5, 11, 22, 29]. However, optimization  
 37 problems (2) for  $p \neq 2$  can be significantly more challenging. For example, for  $p = 1$ ,  
 38 the so-called  $\ell_1$ -regularized problem suffers from non-differentiability at the origin;

---

\*Submitted to the editors Thursday 14th June, 2018.

**Funding:** This work was partially supported by NSF DMS 1654175 and NSF DMS 1723005 (J. Chung) and by EPSRC grant numbers EP/K032208/1 and EP/R014604/1 (J. Chung and S. Gazzola).

<sup>†</sup>Department of Mathematics, Computational Modeling and Data Analytics Division, Academy of Integrated Science, Virginia Tech, Blacksburg, VA, USA (jmchung@vt.edu, <http://www.math.vt.edu/people/jmchung/>).

<sup>‡</sup>Department of Mathematical Sciences, University of Bath, United Kingdom (S.Gazzola@bath.ac.uk, <http://people.bath.ac.uk/sg968/>).

39 moreover, in some situations, one may wish to consider  $0 < p < 1$ , which results  
 40 in a nonconvex optimization problem, see, e.g., [20, 24, 25]. In this paper, we will  
 41 develop methods to compute an approximate solution to (2) for the case  $p \geq 1$ , where  
 42 a unique solution exists. Henceforth, we will refer to problem (2) with  $\Psi = \mathbf{I}$  as the  
 43 “ $\ell_p$ -regularized” problem; problem (2) with  $\Psi \neq \mathbf{I}$  will be dubbed the “transformed  
 44  $\ell_p$ -regularized” problem. Typically the transformed  $\ell_p$ -regularized problem arises in  
 45 cases where sparsity in some frequency domain (e.g., in a wavelet domain) is desired.  
 46 Depending on the application, a sparsity transform may be included in both the fit-  
 47 to-data and the regularization term. This was considered in [33], where the resulting  
 48 minimization problem was solved with an inner-outer iteration scheme.

49 Most of the previously developed methods for  $\ell_p$  minimization utilize nonlinear  
 50 optimization schemes or iteratively reweighted optimization schemes, which can get  
 51 very expensive due to inner-outer iterations [1, 16, 32, 33, 42]. Other popular ap-  
 52 proaches such as the split Bregman method [14], separable approximations [43], and  
 53 accelerations of the iterative shrinkage thresholding algorithms [2] are fast alterna-  
 54 tives, but a main disadvantage is that the regularization parameter must be selected  
 55 a priori, which can be a difficult task. Krylov methods, on the other hand, have nice  
 56 convergence and regularization properties, so there have been recent efforts to exploit  
 57 Krylov methods to solve the  $\ell_p$ -regularized problem, possibly without resorting to  
 58 inner-outer iterations. For example, [20, 24] considered generalized Krylov methods  
 59 for  $\ell_p - \ell_q$  minimization, and Krylov methods based on the flexible Arnoldi algorithm  
 60 were considered in [10, 36, 37]. Our proposed methods are mostly related to the latter  
 61 approaches, which compute approximate solutions to the  $\ell_p$ -regularized problem when  
 62  $\mathbf{A}$  is square. Below we outline the main distinctions and contributions of our work.

63 In this paper, we propose new iterative hybrid methods based on a flexible Golub–  
 64 Kahan decomposition to solve  $\ell_p$ -regularized problems (2), where flexible precondi-  
 65 tioning techniques are used to build appropriate solution subspaces. In particular,  
 66 we describe two methods, namely flexible LSQR and flexible LSMR, and show how  
 67 Tikhonov regularization can be used to solve the projected problem, where the prop-  
 68 erties of the matrices associated with the flexible Golub–Kahan decomposition are  
 69 exploited for efficient regularization parameter selection (in a hybrid fashion). We  
 70 underline that methods based on the flexible Golub–Kahan algorithm can be imple-  
 71 mented without explicitly constructing the matrix  $\mathbf{A}$ , i.e., by treating  $\mathbf{A}$  and  $\mathbf{A}^\top$  as  
 72 linear operators acting on vectors. Furthermore, we describe a way to incorporate  
 73 regularization terms expressed as the  $p$ -norm of the transformed solution within the  
 74 flexible schemes (based on both the Arnoldi and the Golub–Kahan decompositions),  
 75 i.e., to deal with the transformed  $\ell_p$ -regularized problem.

76 One of the first major contributions, compared to [10], is that our methods can be  
 77 used to solve problems with general (e.g., non-square) coefficient matrix  $\mathbf{A}$ . Second, we  
 78 provide theoretical results that show optimality properties for the flexible approaches,  
 79 and we prove that in exact arithmetic flexible LSMR iterates are the same as GM-  
 80 RES iterates on the normal equations. Third, contrary to classical Krylov–Tikhonov  
 81 methods [11], which can handle penalization terms evaluated in the 2-norm, the new  
 82 methods can approximate penalization terms evaluated in the sparsity-inducing 1-  
 83 norm and can include an invertible sparsity transformation, which generalizes the  
 84 flexible Arnoldi decomposition proposed in [10], as well as the flexible Golub–Kahan  
 85 decomposition derived in this paper. Numerical comparisons to well-established  $\ell_1$   
 86 regularization methods reveal that the proposed strategies provide an easy-to-use ap-  
 87 proach for computing reconstructions with similar properties, but with two significant  
 88 benefits: firstly, the regularization parameters can be selected automatically thanks to

89 the hybrid framework; secondly, information from the current solution is incorporated  
 90 via the regularization into the solution process as soon as it becomes available, with  
 91 potentially great computational savings compared to methods involving inner-outer  
 92 iterations.

93 The paper is organized as follows. In Section 2 we review the ideas underlying the  
 94 iteratively reweighted norm (IRN) approach for  $\ell_p$  regularization and briefly review  
 95 the flexible Arnoldi–Tikhonov approach. In Section 3 we derive the flexible Golub–  
 96 Kahan decomposition, leading to the introduction of the new flexible LSQR and  
 97 flexible LSMR algorithms; hybrid approaches based on flexible LSQR and flexible  
 98 LSMR are addressed, with a particular emphasis on the choice of regularization term  
 99 and regularization parameter. Optimality properties for the new solvers and links  
 100 to existing solvers are provided. In Section 4 we describe how a sparsity transform  
 101 can be handled within hybrid schemes based on the flexible Arnoldi and Golub–  
 102 Kahan algorithms, and we investigate how the solution subspaces are modified by  
 103 incorporating reweightings and sparsity transforms. Numerical results are presented  
 104 in Section 5, and conclusions and future work are provided in Section 6.

105 **2. Background on iteratively reweighted and flexible methods for  $\ell_p$**   
 106 **regularization.** A well-established strategy for solving the  $\ell_p$ -regularized problem  
 107 is the iteratively reweighted norm (IRN) algorithm [16, 33]. This approach requires  
 108 solving a sequence of reweighted, penalized least-squares problems where the weights  
 109 change at each iteration. When dealing with large systems, each least-squares problem  
 110 is solved by an iterative method, so that an inner-outer iteration scheme is naturally  
 111 established. In the following we use the acronym IRN to indicate a wide class of  
 112 algorithms that leverage (outer) reweighting together with an (inner) iterative scheme.  
 113 IRN methods are also closely related to iteratively reweighted least squares (IRLS)  
 114 methods [4, Chapter 4]. Since IRN methods can get very costly, another common  
 115 approach is to use iterative shrinkage thresholding algorithms [2], where an iterative  
 116 two-step process is used.

117 Many of these methods assume that a good value of the regularization parameter  
 118 is available *a priori*, but oftentimes this is not the case. And although there have been  
 119 some recent works on selecting regularization parameters for  $\ell_1$  regularization, e.g.,  
 120 [13], these can still be quite costly for very large problems. Selecting regularization  
 121 parameters for  $\ell_p$ -regularized problems remains a tricky, yet crucial, task. For the  
 122 special case where  $p = 2$ , significant works on hybrid methods have enabled successful  
 123 simultaneous estimation of the regularization parameter and computation of large-  
 124 scale reconstructions, see, e.g., [22, 32]. In these hybrid frameworks, the problem is  
 125 projected onto Krylov subspaces of increasing size, and the task of choosing a suitable  
 126 value of the regularization parameter is reduced to solving the smaller, projected  
 127 problem. However, such approaches have not been fully investigated for general  $\ell_p$ -  
 128 regularized problems. The flexible hybrid framework for  $\ell_p$ -regularized problems that  
 129 we describe in Section 3 incorporates simultaneous parameter selection and is based  
 130 on the IRN reformulation.

131 As described in [33], the first step toward an IRN approach is to define a sequence  
 132 of appropriate regularization operators to break the  $\ell_p$ -regularized problem into a  
 133 sequence of 2-norm problems,

$$134 \quad (3) \quad \min_{\mathbf{x}} \|\mathbf{Ax} - \mathbf{b}\|_2^2 + \lambda \|\mathbf{L}(\mathbf{x})\mathbf{x}\|_2^2 ,$$

135 where

$$136 \quad (4) \quad \mathbf{L}(\mathbf{x}) = \text{diag} \left( (|x_i|^{\frac{p-2}{2}})_{i=1, \dots, n} \right).$$

137 Here  $x_i$  is the  $i$ th entry of vector  $\mathbf{x}$ . We remark that, when  $p < 2$ , care is needed  
 138 when defining (4), because division by 0 may occur if  $x_i = 0$  for some  $i = 1, \dots, n$ .  
 139 To fix this potential issue, small thresholds  $\tau_1, \tau_2 > 0$  are set, and the matrix in (4) is  
 140 redefined as

$$141 \quad (5) \quad \mathbf{L}(\mathbf{x}) = \text{diag}((f_\tau(|x_i|)^{\frac{p-2}{2}})_{i=1, \dots, n}), \text{ where } f_\tau(|x_i|) = \begin{cases} |x_i| & \text{if } |x_i| \geq \tau_1, \\ \tau_2 & \text{if } |x_i| < \tau_1. \end{cases}$$

142 Note that taking  $\tau_2 < \tau_1$  enforces additional sparsity in  $f_\tau(|x_i|)$ . In the case  
 143  $p = 1$ , the IRN approach reduces the  $\ell_1$ -regularized problem (2) to a sequence of  
 144 least-squares problems involving a weighted 2-norm. That is,

$$145 \quad \|\mathbf{x}\|_1 \approx \|\mathbf{L}(\mathbf{x})\mathbf{x}\|_2^2,$$

146 where  $\mathbf{L}(\mathbf{x}) = \text{diag}(1/\sqrt{f_\tau(|\mathbf{x}|)})$ ,  $f_\tau(\cdot)$  is defined in (5), and the square root and  
 147 absolute value operations are applied component-wise. We remark that problem (3)  
 148 can be equivalently reformulated as

$$149 \quad (6) \quad \min_{\hat{\mathbf{x}}} \|\mathbf{A}\mathbf{L}(\mathbf{x})^{-1}\hat{\mathbf{x}} - \mathbf{b}\|_2^2 + \lambda \|\hat{\mathbf{x}}\|_2^2,$$

150 where  $\hat{\mathbf{x}} = \mathbf{L}(\mathbf{x})\mathbf{x}$ . This transformation into standard form is computationally conve-  
 151 nient, as it only amounts to the inversion of a diagonal matrix.

152 For realistic scenarios, problems (3) and (6) are intrinsically nonlinear. In order to  
 153 avoid nonlinearities, we follow the common practice of approximating the matrix  $\mathbf{L}(\mathbf{x})$   
 154 by the matrix  $\mathbf{L}_k = \mathbf{L}(\mathbf{x}_k)$ , where  $\mathbf{x}_k$  is an approximation of the solution obtained at  
 155 the  $(k-1)$ st outer iteration. Then at the  $k$ th outer iteration, we solve the Tikhonov  
 156 problem,

$$157 \quad (7) \quad \min_{\mathbf{x}} \|\mathbf{A}\mathbf{x} - \mathbf{b}\|_2^2 + \lambda \|\mathbf{L}_k\mathbf{x}\|_2^2.$$

158 The IRN method proposed in [33] prescribes to apply the conjugate gradient (CG)  
 159 method to solve the normal equations corresponding to (7), i.e.,

$$160 \quad (8) \quad (\mathbf{A}^\top \mathbf{A} + \lambda \mathbf{L}_k^\top \mathbf{L}_k)\mathbf{x} = \mathbf{A}^\top \mathbf{b}, \quad \mathbf{L}_k = \mathbf{L}(\mathbf{x}_k).$$

161 Also preconditioned CG (PCG) can be applied at the  $k$ th outer iteration of IRN to  
 162 solve the normal equations associated to a preconditioned version of (7), i.e.,

$$163 \quad (9) \quad (\mathbf{L}_k^{-\top} \mathbf{A}^\top \mathbf{A} \mathbf{L}_k^{-1} + \lambda \mathbf{I})\hat{\mathbf{x}} = \mathbf{L}_k^{-\top} \mathbf{A}^\top \mathbf{b}, \quad \mathbf{L}_k^{-1}\hat{\mathbf{x}} = \mathbf{x}, \quad \mathbf{L}_k = \mathbf{L}(\mathbf{x}_k).$$

164 We refer to this approach as the preconditioned IRN (PIRN) method, which is simi-  
 165 lar in essence to the inner-outer scheme proposed in [1] to handle total variation  
 166 regularization. We emphasize that the term ‘‘preconditioned’’ is used in a somewhat  
 167 unconventional way: the ‘‘preconditioners’’ considered here are not aimed at accel-  
 168 erating the convergence of the iterative solvers but rather at enforcing some specific  
 169 regularity into the associated solution subspace. Transformed  $\ell_p$ -regularized prob-  
 170 lems can be suitably expressed in this framework too, as we will explain in Section 4.  
 171 We stress once more that, in the IRN framework, the matrix  $\mathbf{L} = \mathbf{L}_k$  changes at each  
 172 outer iteration, resulting in a sequence of least-squares problems to be solved. A more  
 173 efficient alternative that is applied directly to problem (6) and that exploits flexible  
 174 preconditioning to bypass inner-outer iterative schemes is summarized below.

175 *Generalized Arnoldi–Tikhonov approaches.* For completeness, we provide a brief  
 176 overview of the generalized Arnoldi–Tikhonov (GAT) approach [10] to solve problem  
 177 (6), or equivalently problem (3), for  $\mathbf{A} \in \mathbb{R}^{n \times n}$  and for changing preconditioners  
 178  $\mathbf{L}(\mathbf{x}_k) = \mathbf{L}_k$ . Consider the flexibly preconditioned Arnoldi algorithm, in which, at the  
 179  $k$ th iteration, we have

$$180 \quad (10) \quad \mathbf{A}\widehat{\mathbf{Z}}_k = \widehat{\mathbf{V}}_{k+1}\widehat{\mathbf{H}}_k,$$

181 where  $\widehat{\mathbf{H}}_k \in \mathbb{R}^{(k+1) \times k}$  is upper Hessenberg,  $\widehat{\mathbf{V}}_{k+1} = [\widehat{\mathbf{v}}_1 \ \dots \ \widehat{\mathbf{v}}_{k+1}]$  contains or-  
 182 thonormal columns with  $\widehat{\mathbf{v}}_1 = \mathbf{b}/\|\mathbf{b}\|_2$ , and  $\widehat{\mathbf{Z}}_k = [\mathbf{L}_1^{-1}\widehat{\mathbf{v}}_1 \ \dots \ \mathbf{L}_k^{-1}\widehat{\mathbf{v}}_k] \in \mathbb{R}^{n \times k}$ .  
 183 Here and in the following, we assume an initial guess  $\mathbf{x}_0 = \mathbf{0}$ ; extensions to include  
 184  $\mathbf{x}_0 \neq \mathbf{0}$  are trivial and follow standard derivations. Also, throughout the paper, we  
 185 assume that all of the algorithms are breakdown-free, i.e., the dimension of the  $k$ th  
 186 solution subspace is  $k$ . We also note that, if the preconditioner is fixed for all itera-  
 187 tions ( $\mathbf{L}_i = \mathbf{L}$ ,  $i = 1, \dots, k$ ), then  $\widehat{\mathbf{Z}}_k = \mathbf{L}^{-1}\widehat{\mathbf{V}}_k$  and decomposition (10) reduces to the  
 188 one associated with the standard right-preconditioned GMRES method. The GAT  
 189 method computes approximate solutions of the form  $\mathbf{x}_k = \widehat{\mathbf{Z}}_k\widehat{\mathbf{y}}_k$ , where

$$190 \quad (11) \quad \widehat{\mathbf{y}}_k = \arg \min_{\mathbf{y}} \left\| \widehat{\mathbf{H}}_k \mathbf{y} - \|\mathbf{b}\|_2 \mathbf{e}_1 \right\|_2^2 + \lambda \|\mathbf{y}\|_2^2,$$

191 where  $\mathbf{e}_1 \in \mathbb{R}^{k+1}$  is the first column of the identity matrix of order  $k+1$ . For  $\lambda = 0$ ,  
 192 we have the flexible GMRES (FGMRES) method [35]. The main advantages of this  
 193 approach are that *only one* solution subspace needs to be generated (versus multiple  
 194 solves in IRN), one matrix-vector multiplication with  $\mathbf{A}$  is required at each iteration  
 195 (versus one with  $\mathbf{A}$  and one with  $\mathbf{A}^\top$  in CGLS), and a suitable value of the regular-  
 196 ization parameter and an appropriate value of the threshold for the stopping criterion  
 197 are determined automatically by exploiting the hybrid framework. In [10], the GAT  
 198 method and its variants were used to efficiently compute approximate solutions to  
 199  $\ell_1$ -regularized problems, but a limitation is that this method only works for square  
 200 problems. A naïve extension of the GAT method to general least-squares problems by  
 201 applying the flexible Arnoldi algorithm to the normal equations is not recommended,  
 202 due to the squaring of the condition number of the coefficient matrix and the lack  
 203 of a computationally convenient way to estimate the residual norm for the original  
 204 problem (1). Although flexible versions of the so-called AB-GMRES and BA-GMRES  
 205 methods [26] may be devised, in the following section we exploit a new computational  
 206 tool from numerical linear algebra, namely the flexible Golub–Kahan method. In this  
 207 way, we avoid the normal equations and work directly with the residual from the  
 208 original least-squares problem, which can be helpful in determining the regularization  
 209 parameter and stopping criteria.

210 **3. Flexible Golub–Kahan hybrid methods.** In this section, we describe hy-  
 211 brid approaches based on the flexible Golub–Kahan process for computing an approxi-  
 212 mate solution to the Tikhonov problem (7), where  $\mathbf{L}_k$  may change at each iteration. As  
 213 discussed in Section 2, problem (7) approximates regularized problem (3). Similarly  
 214 to the GAT method, the flexible Golub–Kahan hybrid methods follow an iterative  
 215 two-step process. First we generate a basis for the solution by exploiting a flexible  
 216 preconditioning framework to take into account a changing regularizer, and second,  
 217 we compute an approximate solution to the inverse problem by solving an optimiza-  
 218 tion problem in the projected subspace (where regularization can be done efficiently  
 219 and with automatic regularization parameter selection for the projected problem).

220 These iterative approaches are ideal for problems where  $\mathbf{A}$  and  $\mathbf{A}^\top$  can be accessed  
 221 only by matrix-vector multiplication, where only a few basis vectors are required to  
 222 obtain a good solution, and where a suitable value of the regularization parameter is  
 223 not known a priori.

224 **3.1. Incorporating weights: a flexible Golub–Kahan decomposition.** In  
 225 order to incorporate a changing preconditioner, we use a flexible variant of the Golub–  
 226 Kahan bidiagonalization (GKB) algorithm to generate a basis for the solution. We call  
 227 this the *flexible Golub–Kahan* (FGK) process, and mention that it is closely related  
 228 to the inexact Lanczos process [38, 41]. Given  $\mathbf{A}$ ,  $\mathbf{b}$ , and changing preconditioners  
 229  $\mathbf{L}_k$ , the  $k$ th iteration of the FGK iterative process generates vectors  $\mathbf{z}_k$ ,  $\mathbf{v}_k$ , and  $\mathbf{u}_{k+1}$   
 230 such that

$$231 \quad (12) \quad \mathbf{A}\mathbf{Z}_k = \mathbf{U}_{k+1}\mathbf{M}_k \quad \text{and} \quad \mathbf{A}^\top\mathbf{U}_{k+1} = \mathbf{V}_{k+1}\mathbf{T}_{k+1},$$

232 where

- 233 •  $\mathbf{Z}_k = [\mathbf{z}_1 \ \cdots \ \mathbf{z}_k] = [\mathbf{L}_1^{-1}\mathbf{v}_1 \ \cdots \ \mathbf{L}_k^{-1}\mathbf{v}_k] \in \mathbb{R}^{n \times k}$ ,
- 234 •  $\mathbf{M}_k = [m_{i,j}]_{i=1,\dots,k+1;j=1,\dots,k} \in \mathbb{R}^{(k+1) \times k}$  is upper Hessenberg,
- 235 •  $\mathbf{T}_{k+1} = [t_{i,j}]_{i,j=1,\dots,k+1} \in \mathbb{R}^{(k+1) \times (k+1)}$  is upper triangular,
- 236 •  $\mathbf{U}_{k+1} = [\mathbf{u}_1 \ \cdots \ \mathbf{u}_{k+1}] \in \mathbb{R}^{m \times (k+1)}$  has orthonormal columns with  $\mathbf{u}_1 = \mathbf{b}/\|\mathbf{b}\|_2$ , and
- 237 •  $\mathbf{V}_{k+1} = [\mathbf{v}_1 \ \cdots \ \mathbf{v}_{k+1}] \in \mathbb{R}^{n \times (k+1)}$  has orthonormal columns.

238 Compared to standard GKB [15], the key differences are that we now have an  
 239 upper Hessenberg and an upper triangular matrix, instead of one bidiagonal matrix.  
 240 Also, we must keep track of an additional set of vectors, namely the basis vectors  
 241 in  $\mathbf{Z}_k$ . Furthermore, since there is no bidiagonal structure to exploit, the additional  
 242 computational requirement is orthogonalization with all previous vectors. However,  
 243 these additional requirements are negligible if  $k \ll \max\{m, n\}$ . Moreover, as for  
 244 standard GKB, the computational cost per iteration is dominated by a matrix-vector  
 245 product with  $\mathbf{A}$  and one with  $\mathbf{A}^\top$ . We remark that, if  $\mathbf{L}_k = \mathbf{L}$ , (12) reduces to the  
 246 right-preconditioned GKB. The FGK process is summarized in Algorithm 1.

---

**Algorithm 1** Flexible Golub–Kahan (FGK) Process

---

- 1: Initialize  $\mathbf{u}_1 = \mathbf{b}/\beta_1$ , where  $\beta_1 = \|\mathbf{b}\|$
  - 2: **for**  $i = 1, \dots, k$  **do**
  - 3:    $\mathbf{w} = \mathbf{A}^\top\mathbf{u}_i$ ,  $t_{j,i} = \mathbf{w}^\top\mathbf{v}_j$  for  $j = 1, \dots, i-1$
  - 4:    $\mathbf{w} = \mathbf{w} - \sum_{j=1}^{i-1} t_{j,i}\mathbf{v}_j$ ,  $t_{i,i} = \|\mathbf{w}\|$ ,  $\mathbf{v}_i = \mathbf{w}/t_{i,i}$
  - 5:    $\mathbf{z}_i = \mathbf{L}_i^{-1}\mathbf{v}_i$
  - 6:    $\mathbf{w} = \mathbf{A}\mathbf{z}_i$ ,  $m_{j,i} = \mathbf{w}^\top\mathbf{u}_j$  for  $j = 1, \dots, i$
  - 7:    $\mathbf{w} = \mathbf{w} - \sum_{j=1}^i m_{j,i}\mathbf{u}_j$ ,  $m_{i+1,i} = \|\mathbf{w}\|$ ,  $\mathbf{u}_{i+1} = \mathbf{w}/m_{i+1,i}$
  - 8: **end for**
- 

247 Notice that the column vectors of  $\mathbf{Z}_k$  no longer span a Krylov subspace in a  
 248 traditional sense, but they do provide a basis for the solution subspace. In Section  
 249 5 we provide some qualitative observations regarding the basis vectors. For now,  
 250 consider the fit-to-data term  $\|\mathbf{A}\mathbf{x} - \mathbf{b}\|_2^2$  and consider solutions in the column space  
 251 of  $\mathbf{Z}_k$ , denoted by  $\mathcal{R}(\mathbf{Z}_k)$ . Using the relationships in (12), the residual can be written  
 252 as

$$253 \quad \mathbf{A}\mathbf{Z}_k\mathbf{y} - \mathbf{b} = \mathbf{U}_{k+1}(\mathbf{M}_k\mathbf{y} - \beta_1\mathbf{e}_1).$$

254 We define the flexible LSQR (FLSQR) and flexible LSMR (FLSMR) iterates as



255  $\mathbf{x}_k = \mathbf{Z}_k \mathbf{y}_k$ , where

$$256 \quad (13) \quad \mathbf{y}_k = \arg \min_{\mathbf{y}} \|\mathbf{M}_k \mathbf{y} - \beta_1 \mathbf{e}_1\|_2^2$$

257 and

$$258 \quad (14) \quad \mathbf{y}_k = \arg \min_{\mathbf{y}} \|\mathbf{T}_{k+1} \mathbf{M}_k \mathbf{y} - \beta_1 t_{1,1} \mathbf{e}_1\|_2^2,$$

259 respectively. These definitions are analogous to the mathematical definitions of the  
260 LSQR and LSMR iterates in [8, 30, 31]. The FLSMR formulation exploits the follow-  
261 ing relationships

$$262 \quad \mathbf{A}^\top (\mathbf{A} \mathbf{Z}_k \mathbf{y} - \mathbf{b}) = \mathbf{V}_{k+1} (\mathbf{T}_{k+1} \mathbf{M}_k \mathbf{y} - t_{1,1} \beta_1 \mathbf{e}_1) \quad \text{and} \quad \mathbf{A}^\top \mathbf{b} = \mathbf{V}_{k+1} \beta_1 t_{1,1} \mathbf{e}_1.$$

263 We have the following optimality properties for FLSQR and FLSMR, which are  
264 analogous to the ones enjoyed by the standard counterparts of these methods and by  
265 FGMRES [35].

266 PROPOSITION 3.1. *The FLSQR iterate  $\mathbf{x}_k$  obtained at the  $k$ th step minimizes the*  
267 *residual norm  $\|\mathbf{A} \mathbf{x}_k - \mathbf{b}\|_2$  over  $\mathcal{R}(\mathbf{Z}_k)$ , and the FLSMR iterate  $\mathbf{x}_k$  obtained at the*  
268  *$k$ th step minimizes  $\|\mathbf{A}^\top (\mathbf{A} \mathbf{x}_k - \mathbf{b})\|_2$  over  $\mathcal{R}(\mathbf{Z}_k)$ .*

269 We note that FLSQR is mathematically equivalent to the full-recurrence flexible  
270 conjugate gradient method [28] applied to the normal equations, but the advantages  
271 of this formulation are that we avoid working directly with the normal equations,  
272 and there is a natural means to evaluate residuals for the original system. In this  
273 respect, FLSQR is comparable to the FCGLS method in [12]. Furthermore, we note  
274 that  $\mathbf{T}_{k+1} \mathbf{M}_k$  is a  $(k+1) \times k$  upper Hessenberg matrix and that the solution subspace  
275 generated by the FGK process is the same as the one generated by the flexible Arnoldi  
276 algorithm applied to the normal equations. More precisely, the following equivalence  
277 theorem holds.

278 THEOREM 3.2. *Let  $\mathbf{A} \in \mathbb{R}^{m \times n}$ ,  $m \geq n$  and take the preconditioners  $\mathbf{L}_i$ ,*  
279  *$i = 1, 2, \dots, k$ . Then, in exact arithmetic, the  $k$ th iterate of FLSQR applied to*  
280  *$\min_{\mathbf{x}} \|\mathbf{A} \mathbf{x} - \mathbf{b}\|_2$  is equivalent to the  $k$ th iterate of FCGLS applied to the same problem;*  
281 *moreover, the  $k$ th iterate of FLSMR applied to  $\min_{\mathbf{x}} \|\mathbf{A} \mathbf{x} - \mathbf{b}\|_2$  is equivalent to the*  
282  *$k$ th iterate of FGMRES applied to the normal equations*

$$283 \quad (15) \quad \mathbf{A}^\top \mathbf{A} \mathbf{x} = \mathbf{A}^\top \mathbf{b}.$$

284 *Proof.* Directly from Algorithm 1 and [12, Algorithm 1], the iterates computed  
285 by both FLSQR and FCGLS are such that

$$\begin{aligned} 286 \quad \mathbf{x}_1 &\in \text{span}\{\mathbf{L}_1^{-1} \mathbf{A}^\top \mathbf{b}\}, \\ \mathbf{x}_2 &\in \text{span}\{\mathbf{L}_2^{-1} \mathbf{A}^\top \mathbf{b}, \mathbf{L}_2^{-1} \mathbf{A}^\top \mathbf{A} \mathbf{L}_1^{-1} \mathbf{A}^\top \mathbf{b}, \mathbf{x}_1\}, \\ \mathbf{x}_3 &\in \text{span}\{\mathbf{L}_3^{-1} \mathbf{A}^\top \mathbf{b}, \mathbf{L}_3^{-1} \mathbf{A}^\top \mathbf{A} \mathbf{L}_1^{-1} \mathbf{A}^\top \mathbf{b}, \mathbf{L}_3^{-1} \mathbf{A}^\top \mathbf{A} \mathbf{L}_2^{-1} \mathbf{A}^\top \mathbf{b}, \\ &\quad \mathbf{L}_3^{-1} \mathbf{A}^\top \mathbf{A} \mathbf{L}_2^{-1} \mathbf{A}^\top \mathbf{A} \mathbf{L}_1^{-1} \mathbf{A}^\top \mathbf{b}, \mathbf{x}_2\}, \\ &\dots \end{aligned}$$

287 Since both the FLSQR and the FCGLS iterates minimize the residual norm over the  
288 same solution subspace, we can conclude that FLSQR is mathematically equivalent  
289 to FCGLS. Concerning the second part of the statement, note that after  $k$  iterations  
290 of FGMRES applied to (15), we have a matrix  $\hat{\mathbf{Z}}_k = [\mathbf{L}_1^{-1} \hat{\mathbf{v}}_1 \quad \dots \quad \mathbf{L}_k^{-1} \hat{\mathbf{v}}_k] \in \mathbb{R}^{n \times k}$ ,



291 an upper Hessenberg matrix  $\widehat{\mathbf{H}}_k \in \mathbb{R}^{(k+1) \times k}$ , and a matrix  $\widehat{\mathbf{V}}_{k+1} \in \mathbb{R}^{n \times (k+1)}$  with  
 292 orthonormal columns and  $\widehat{\mathbf{V}}_{k+1} \mathbf{e}_1 = \mathbf{A}^\top \mathbf{b} / \|\mathbf{A}^\top \mathbf{b}\|_2$ , which satisfy the relationship

$$293 \quad (16) \quad \mathbf{A}^\top \mathbf{A} \widehat{\mathbf{Z}}_k = \widehat{\mathbf{V}}_{k+1} \widehat{\mathbf{H}}_k.$$

294 The projected problem is given by

$$295 \quad (17) \quad \min_{\mathbf{x} \in \mathcal{R}(\widehat{\mathbf{Z}}_k)} \|\mathbf{A}^\top \mathbf{A} \mathbf{x} - \mathbf{A}^\top \mathbf{b}\|_2^2 = \min_{\mathbf{y}} \left\| \widehat{\mathbf{H}}_k \mathbf{y} - \|\mathbf{A}^\top \mathbf{b}\|_2 \mathbf{e}_1 \right\|_2^2,$$

296 so the  $k$ th iterate of FGMRES is given by

$$297 \quad \widehat{\mathbf{x}}_k = \widehat{\mathbf{Z}}_k \widehat{\mathbf{H}}_k^\dagger \|\mathbf{A}^\top \mathbf{b}\|_2 \mathbf{e}_1,$$

298 where  $\widehat{\mathbf{H}}_k^\dagger = (\widehat{\mathbf{H}}_k^\top \widehat{\mathbf{H}}_k)^{-1} \widehat{\mathbf{H}}_k^\top$  is the pseudoinverse. In exact arithmetic the solution  
 299 subspaces generated by FGMRES and FGK in Algorithm 1 are the same, and coincide  
 300 with

$$301 \quad \text{span}\{\mathbf{L}_1^{-1} \widehat{\mathbf{v}}_1, \mathbf{L}_2^{-1} \widehat{\mathbf{v}}_2, \dots, \mathbf{L}_k^{-1} \widehat{\mathbf{v}}_k\},$$

302 so that  $\widehat{\mathbf{Z}}_k = \mathbf{Z}_k$  (this is immediate from factorizations (12) and (16)). The optimality  
 303 condition for FGMRES (see Proposition 2.1 in [35]) and FLSMR (see Proposition 3.1)  
 304 guarantee that the  $k$ th iterate of FLSMR and FGMRES both correspond to the  
 305 solution of (17).  $\square$

306 **3.2. Solving the regularized problem: flexible hybrid algorithms.** As  
 307 explained in Section 3.1, the FGK process can be used to build a solution subspace  
 308 that can efficiently incorporate changing preconditioners, and one can solve the pro-  
 309 jected problems (13) and (14), which correspond to the FLSQR and FLSMR methods,  
 310 respectively. However, it is well-known that, for inverse problems, iterative meth-  
 311 ods exhibit a semiconvergent behavior, where the relative reconstruction error norm  
 312  $\|\mathbf{x}_k - \mathbf{x}_{\text{true}}\|_2 / \|\mathbf{x}_{\text{true}}\|_2$  decreases initially but at some point increases due to ampli-  
 313 fication of noise [18]. This phenomenon, which is common for most ill-posed inverse  
 314 problems, occurs also for flexible methods, as can be seen in Figure 1(a).

315 Hybrid methods, where regularization is included on the projected problem, have  
 316 been proposed to suppress the relative reconstruction error norms, i.e., to mitigate  
 317 semiconvergence. The first hybrid approach that we propose is analogous to the GAT  
 318 algorithm (see (11)), where we include a standard regularization term in (13), so that

$$319 \quad (18) \quad \mathbf{y}_k = \arg \min_{\mathbf{y}} \|\mathbf{M}_k \mathbf{y} - \beta_1 \mathbf{e}_1\|_2^2 + \lambda \|\mathbf{y}\|_2^2.$$

320 Henceforth, we define FLSQR-I iterates as  $\mathbf{x}_k = \mathbf{Z}_k \mathbf{y}_k$ , where  $\mathbf{y}_k$  is defined in (18).

321 Let  $\mathbf{Z}_k = \mathbf{Q}_k \mathbf{R}_k$  be the thin QR factorization of  $\mathbf{Z}_k$  where  $\mathbf{R}_k \in \mathbb{R}^{k \times k}$  is upper  
 322 triangular and  $\mathbf{Q}_k \in \mathbb{R}^{n \times k}$  contains orthonormal columns. This is inexpensive to  
 323 compute if  $k$  is not too large. Then we also consider a hybrid method called FLSQR-  
 324 R, in which iterates are constructed as  $\mathbf{x}_k = \mathbf{Z}_k \mathbf{y}_k$ , where

$$325 \quad (19) \quad \mathbf{y}_k = \arg \min_{\mathbf{y}} \|\mathbf{M}_k \mathbf{y} - \beta_1 \mathbf{e}_1\|_2^2 + \lambda \|\mathbf{R}_k \mathbf{y}\|_2^2.$$

326 The FLSQR-R method exhibits some desirable properties, especially for inverse prob-  
 327 lems. First, the FLSQR-R iterate can be interpreted as a best approximation in a

328 subspace, in that  $\mathbf{x}_k$  solves

329 (20) 
$$\min_{\mathbf{x} \in \mathcal{R}(\mathbf{Z}_k)} \|\mathbf{A}\mathbf{x} - \mathbf{b}\|_2^2 + \lambda \|\mathbf{x}\|_2^2.$$

330 Hence, the regularization parameter  $\lambda$ , which specifies the amount of regularization  
 331 for the projected problem (19), corresponds to the amount of regularization for the  
 332 constrained, full-dimensional problem (20). Second, using the following reformulation  
 333 of the FLSQR-R subproblem (19),

334 
$$\mathbf{w}_k = \arg \min_{\mathbf{w}} \|\mathbf{M}_k \mathbf{R}_k^{-1} \mathbf{w} - \beta_1 \mathbf{e}_1\|_2^2 + \lambda \|\mathbf{w}\|_2^2, \quad \mathbf{y}_k = \mathbf{R}_k^{-1} \mathbf{w}_k,$$

335 we can show that the singular values of the coefficient matrix  $\mathbf{M}_k \mathbf{R}_k^{-1}$  provide good  
 336 approximations to the singular values of  $\mathbf{A}$ . Indeed, we can see this by considering the  
 337 following relations (where decomposition (12) and properties of the matrices appearing  
 338 therein are extensively used):

339 
$$\begin{aligned} \mathbf{R}_k^{-\top} \mathbf{M}_k^{\top} \mathbf{M}_k \mathbf{R}_k^{-1} &= \mathbf{R}_k^{-\top} \mathbf{M}_k^{\top} \mathbf{U}_{k+1}^{\top} \mathbf{U}_{k+1} \mathbf{M}_k \mathbf{R}_k^{-1} \\ 340 &= \mathbf{R}_k^{-\top} \mathbf{Z}_k^{\top} \mathbf{A}^{\top} \mathbf{A} \mathbf{Z}_k \mathbf{R}_k^{-1} \\ 341 &= \mathbf{Q}_k^{\top} \mathbf{A}^{\top} \mathbf{A} \mathbf{Q}_k. \end{aligned}$$

343 Since the eigenvalues are just the squares of the singular values, we see that as  $k$   
 344 increases, the singular values of  $\mathbf{M}_k \mathbf{R}_k^{-1}$  provide better approximations to the singular  
 345 values of  $\mathbf{A}$ .

346 Hybrid LSMR variants, namely the FLSMR-I and FLSMR-R methods, can be  
 347 defined analogously. Then, using Theorem 3.2, we can see that in exact arithmetic and  
 348 for a fixed regularization parameter, the FLSMR-I iterates are the same as the GAT  
 349 iterates applied to a Tikhonov problem with the fit-to-data term  $\|\mathbf{A}^{\top} \mathbf{A} \mathbf{x} - \mathbf{A}^{\top} \mathbf{b}\|_2^2$ .  
 350 However, the benefit of the FGK approaches versus GAT on the normal equations is  
 351 that FGK produces residual norms for the original problem, which can be important  
 352 for tools such as the discrepancy principle for parameter selection and for stopping  
 353 criteria.

354 Unless otherwise stated, the parameter choice methods considered here are based  
 355 on the discrepancy principle: in particular, we either prescribe the discrepancy prin-  
 356 ciple to be satisfied at each iteration, or we apply the ‘‘secant update’’ variant pre-  
 357 scribing suitable updates of the regularization parameter at each iteration. More  
 358 specifically, we determine an appropriate combination of regularization parameters  
 359 (i.e., the number of performed iterations  $k$  and the Tikhonov parameter  $\lambda > 0$ ) such  
 360 that

361 (21) 
$$\|\mathbf{b} - \mathbf{A}\mathbf{x}_k\|_2 \leq \eta \|\mathbf{e}\|_2,$$

362 where  $\mathbf{x}_k$  solves (20) and depends on both  $k$  and  $\lambda$ , and  $\eta > 1$  is a safety factor.  
 363 See [10] and [11] for a detailed description of these regularization parameter selection  
 364 and stopping criteria strategies.

365 *An Illustration.* The goals of this illustration are (i) to demonstrate the higher  
 366 quality of the solutions obtained by applying flexible methods (due to a better basis  
 367 for the solution subspace), (ii) to motivate the need for a hybrid approach (by showing  
 368 semiconvergence behavior of FLSQR and FLSMR), and (iii) to show that the singular  
 369 values of the original problem can be approximated well by using FLSQR-R. More  
 370 thorough numerical results and comparisons will be presented in Section 5.

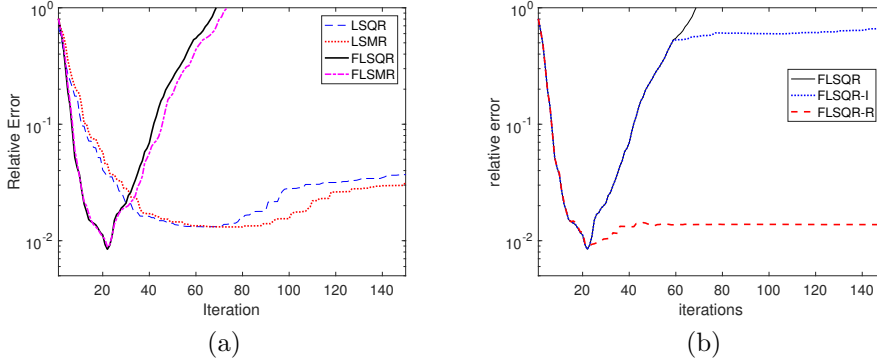


FIG. 1. **heat** test problem from [17]. (a) relative error norm,  $\|\mathbf{x}_k - \mathbf{x}_{\text{true}}\|_2 / \|\mathbf{x}_{\text{true}}\|_2$ , for LSQR, LSMR, FLSQR, and FLSMR. The semiconvergence behavior is evident for all of the methods. (b) relative error norms for FLSQR-I and FLSQR-R with optimal regularization parameters, along with relative error norms for FLSQR provided for comparison.

371 For this illustration, we use the **heat** example from *Regularization Tools* [17],  
 372 where  $\mathbf{A}$  has size  $512 \times 512$ , having a sparse true solution (50% of its entries are zero,  
 373 so that  $\Psi = \mathbf{I}$  and  $p = 1$  in (2)). White noise is added to the observed signal at  
 374 noise level  $10^{-4}$ , i.e.,  $\|\mathbf{b}\|_2 / \|\mathbf{A}\mathbf{x}_{\text{true}}\|_2 = 10^{-4}$ . In Figure 1(a), we provide relative re-  
 375 construction error norms per iteration for LSQR, LSMR, FLSQR, and FLSMR. The  
 376 delayed semiconvergence of LSMR versus LSQR was noted in [5] and is also slightly  
 377 visible for FLSMR versus FLSQR. The more pronounced feature that we see here is  
 378 that the flexible variants converge faster but also exhibit stronger semiconvergence  
 379 in that the relative error norms increase faster. Thus, there is a greater need for  
 380 additional regularization. In Figure 1(b), we show that the hybrid methods FLSQR-I  
 381 and FLSQR-R (here with the optimal regularization parameters, i.e., the ones that  
 382 minimize the relative error norm at each iteration) can mitigate the semiconvergence  
 383 behavior. Comparisons with different parameter selection methods can be found in  
 384 Section 5. We note that, for this particular test problem, flexible preconditioning  
 385 speeds up the convergence of the iterative method. However, for our problems of  
 386 interest (e.g.,  $\ell_p$ -regularized problems), flexible preconditioning is mainly used to im-  
 387 prove the solution subspace. Thus, the particular choice of regularization for the  
 388 projected problem is not so critical and is mostly required for suppressing the errors.

389 Another important tool for the analysis of a regularization method is the ap-  
 390 proximation of the singular values of  $\mathbf{A}$ . For the standard GKB algorithm, it is well  
 391 known that the singular values of the bidiagonal matrix approximate the singular  
 392 values of  $\mathbf{A}$  [34]. However, these results do not directly extend to the FGK process.  
 393 In Figure 2, we display the singular values of  $\mathbf{A}$  with a dashed line, which is partially  
 394 covered by the FLSQR-R curve (continuous asterisked line). Then, for  $k = 20$  to  
 395  $k = 420$  in intervals of 100, we provide the singular values of upper Hessenberg ma-  
 396 trix  $\mathbf{M}_k$  for FLSQR (continuous circled line) and FLSQR-I (continuous squared line),  
 397 and the singular values of  $\mathbf{M}_k \mathbf{R}_k^{-1}$  for FLSQR-R. Note that, in the flexible methods,  
 398 the previous iterate  $\mathbf{x}_{k-1}$ , which may include regularization, changes the precondi-  
 399 tioner and hence the FGK matrices. It is evident that singular values of  $\mathbf{M}_k \mathbf{R}_k^{-1}$  from  
 400 FLSQR-R provide better approximations to the singular values of  $\mathbf{A}$  than those of  
 401  $\mathbf{M}_k$  from FLSQR and FLSQR-I. Furthermore, with more iterations, smaller singular  
 402 values of  $\mathbf{A}$  are being approximated, which motivates the need for regularization of

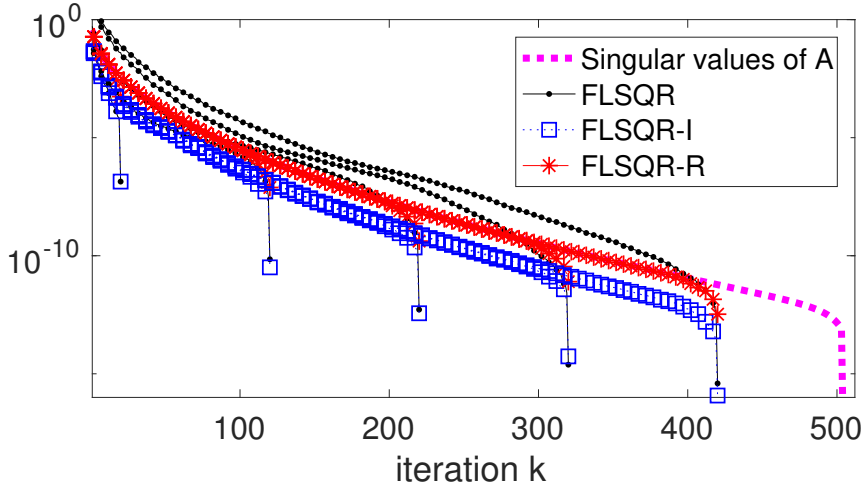


FIG. 2. heat test problem from [17]. This plot compares the singular values of  $\mathbf{A}$  to the singular values of  $\mathbf{M}_k$  from *FLSQR* and *FLSQR-I* and to the singular values of  $\mathbf{M}_k \mathbf{R}_k^{-1}$  from *FLSQR-R*, for iterations  $k$  between 20 and 420 in increments of 100.

403 the projected problem.

404 **4. Flexible methods for the transformed problem.** As mentioned in Sec-  
 405 tion 1, the goal in many applications is to compute solutions that are sparse with  
 406 respect to some transformation (e.g., in a frequency domain). In this section, we  
 407 focus on flexible Arnoldi and flexible Golub–Kahan hybrid methods for solving the  
 408 transformed  $\ell_p$ -regularized problem (2) where  $\Psi \neq \mathbf{I}$ . Although any invertible trans-  
 409 form matrix can be used here, we will focus on wavelet transforms mainly for two  
 410 reasons. Firstly, it is well known that many images can be sparsely represented in the  
 411 wavelet domain. Indeed, wavelet-based iterative methods have been widely considered  
 412 for linear inverse problems, see, e.g., [6, 7, 23, 40]. Secondly, when taking orthonor-  
 413 mal wavelet transforms, computations involving 2-norms of transformed quantities or  
 414 inverse transforms can be easily performed. The specific strategy used to incorporate  
 415 a wavelet transform into the flexible iterative solvers depends on the properties of the  
 416 linear system at hand (which, eventually, depends on the properties of the inverse  
 417 problem to be regularized) and, for all the methods, the regularization parameter can  
 418 be automatically estimated.

419 Let  $\tilde{\Psi} \in \mathbb{R}^{m \times m}$  be an orthogonal matrix. Then, problem (2) is equivalent to

$$420 \quad (22) \quad \min_{\mathbf{x}} \left\| \tilde{\Psi} \mathbf{A} \Psi^{-1} \Psi \mathbf{x} - \tilde{\Psi} \mathbf{b} \right\|_2^2 + \lambda \|\Psi \mathbf{x}\|_p^p.$$

421 Moreover, after some variable transformations, (22) can be written as

$$422 \quad (23) \quad \min_{\mathbf{s}} \|\mathbf{H} \mathbf{s} - \mathbf{d}\|_2^2 + \lambda \|\mathbf{s}\|_p^p, \quad \text{where } \mathbf{H} = \tilde{\Psi} \mathbf{A} \Psi^{-1}, \mathbf{s} = \Psi \mathbf{x}, \mathbf{d} = \tilde{\Psi} \mathbf{b},$$

423 which is an  $\ell_p$ -regularized problem. The choice of  $\tilde{\Psi}$  is problem-dependent and solver-  
 424 dependent. For instance, when considering image deblurring problems where both  $\mathbf{x}$   
 425 and  $\mathbf{b}$  are images of the same size described by pixel values, it is natural to take

426  $\tilde{\Psi} = \Psi$  to be an orthogonal wavelet transform; this formulation was considered in [3].  
 427 If the GAT method is applied to problem (23) with  $p = 1$  and variable preconditioner  $\mathbf{L}(\mathbf{s}_k) = \mathbf{L}_k$ , then the subspace  $\mathcal{S}_k = \text{span}\{\mathbf{L}_1^{-1}\hat{\mathbf{v}}_1, \mathbf{L}_2^{-1}\hat{\mathbf{v}}_2, \dots, \mathbf{L}_k^{-1}\hat{\mathbf{v}}_k\}$ , with  
 428  $\hat{\mathbf{v}}_1 = \mathbf{d}/\|\mathbf{d}\|_2$ , is generated for the  $k$ th approximation of the transformed solution  $\mathbf{s}$ .  
 429 This subspace enforces sparsity in the wavelet domain for the wavelet coefficients  $\mathbf{s}$  of  
 430 the original image  $\mathbf{x}$ . The solution subspace for the latter is given by  $\Psi^\top \mathcal{S}_k$ , so that  
 431 it is evident that first sparsity is enforced in the wavelet domain, and then the sparse  
 432 wavelet coefficients are transformed back into the original pixel domain. However, for  
 433 situations where one has no intuition regarding the sparsity properties of  $\mathbf{b}$ , one can  
 434 simply take  $\tilde{\Psi} = \mathbf{I}$ . Analogously, if solvers based on the FGK process are applied to  
 435 solve the same problem, then the solution subspace is given by

$$437 \quad \Psi^\top \text{span}\{\mathbf{L}_1^{-1}\Psi\mathbf{v}_1, \dots, \mathbf{L}_k^{-1}\Psi\mathbf{v}_k\}, \quad \text{with } \mathbf{v}_1 = \mathbf{A}^\top \mathbf{b} / \|\mathbf{A}^\top \mathbf{b}\|_2.$$

438 Notice that the choice of  $\tilde{\Psi}$  is irrelevant for flexible methods based on FGK, since

$$439 \quad \mathbf{H}^\top \mathbf{d} = \Psi \mathbf{A}^\top \tilde{\Psi}^\top \tilde{\Psi} \mathbf{b} = \Psi \mathbf{A}^\top \mathbf{b}, \quad \mathbf{H}^\top \mathbf{H} = \Psi \mathbf{A}^\top \tilde{\Psi}^\top \tilde{\Psi} \mathbf{A} \Psi^\top = \Psi \mathbf{A}^\top \mathbf{A} \Psi^\top.$$

440 *An Illustration.* The goal of this illustration is to show that the solution space  
 441 generated by the flexible Arnoldi algorithm applied to problem (23) is more suitable  
 442 than the one generated by its standard counterpart. We consider a 1D signal  $\mathbf{x}$  with  
 443 64 entries, generated in such a way that only 8 of its 1-level Haar wavelet coefficients  
 444  $\mathbf{s}$  are nonzero. The signal is corrupted by Gaussian blur with variance 2.25 and  
 445 band 5, and white noise of level  $10^{-2}$  is added. The exact and corrupted signals  
 446 are displayed in Figure 3(a), and their wavelet coefficients are displayed in Figure  
 447 3(b). We choose  $\lambda = 0$  in (23) so that the solution subspace does not depend on the  
 448 specific parameter choice strategy that one may wish to consider. The threshold  $\tau_1$   
 449 in (5) is set to 0.2, while  $\tau_2 = 10^{-14}$ . Figure 3(c) displays the best reconstructions  
 450 obtained by the FGMRES (11th iteration) and the GMRES (30th iteration) methods.  
 451 One can clearly see that the FGMRES solution is of much higher quality than the  
 452 GMRES one, and that the wavelet coefficients of the FGMRES solution are much  
 453 sparser than the GMRES ones (see Figure 3(d)). The good performance of FGMRES  
 454 for this example can be explained by looking at some of the basis vectors for the  
 455 solution space, displayed in Figure 3(e)–(h). Indeed, the preconditioned basis vectors  
 456 for the signal  $\mathbf{x}$  have a piecewise-constant behavior, while the unpreconditioned ones  
 457 display spurious oscillations; correspondingly, the preconditioned basis vectors for the  
 458 wavelet coefficients  $\mathbf{s}$  have a clear sparsity pattern, which is not reproduced by the  
 459 unpreconditioned ones. Therefore, the FGMRES solution is better than the GMRES  
 460 one as it is obtained by combining better basis vectors for the solution subspace. We  
 461 remark that the basis vectors generated from the FGK process have similar properties,  
 462 and thus are omitted. Also, a similar behavior of the preconditioned basis vectors can  
 463 be observed in the more challenging experiments presented in Section 5.

464 **5. Numerical Results.** In this section, we provide three experiments to demon-  
 465 strate the performance of the flexible Krylov hybrid methods on various test problems  
 466 from image processing. The first two experiments are examples from image deblurring,  
 467 where enforcing sparsity on the image and sparsity on the wavelet coefficients  
 468 are investigated separately. The third experiment is concerned with tomographic  
 469 reconstruction from undersampled data, where sparsity is imposed on the wavelet  
 470 coefficients. All images are of size  $256 \times 256$  pixels. For all of the experiments, the  
 471 thresholds in (5) are  $\tau_1 = 10^{-10}$ ,  $\tau_2 = 10^{-16}$  (machine precision). All experiments

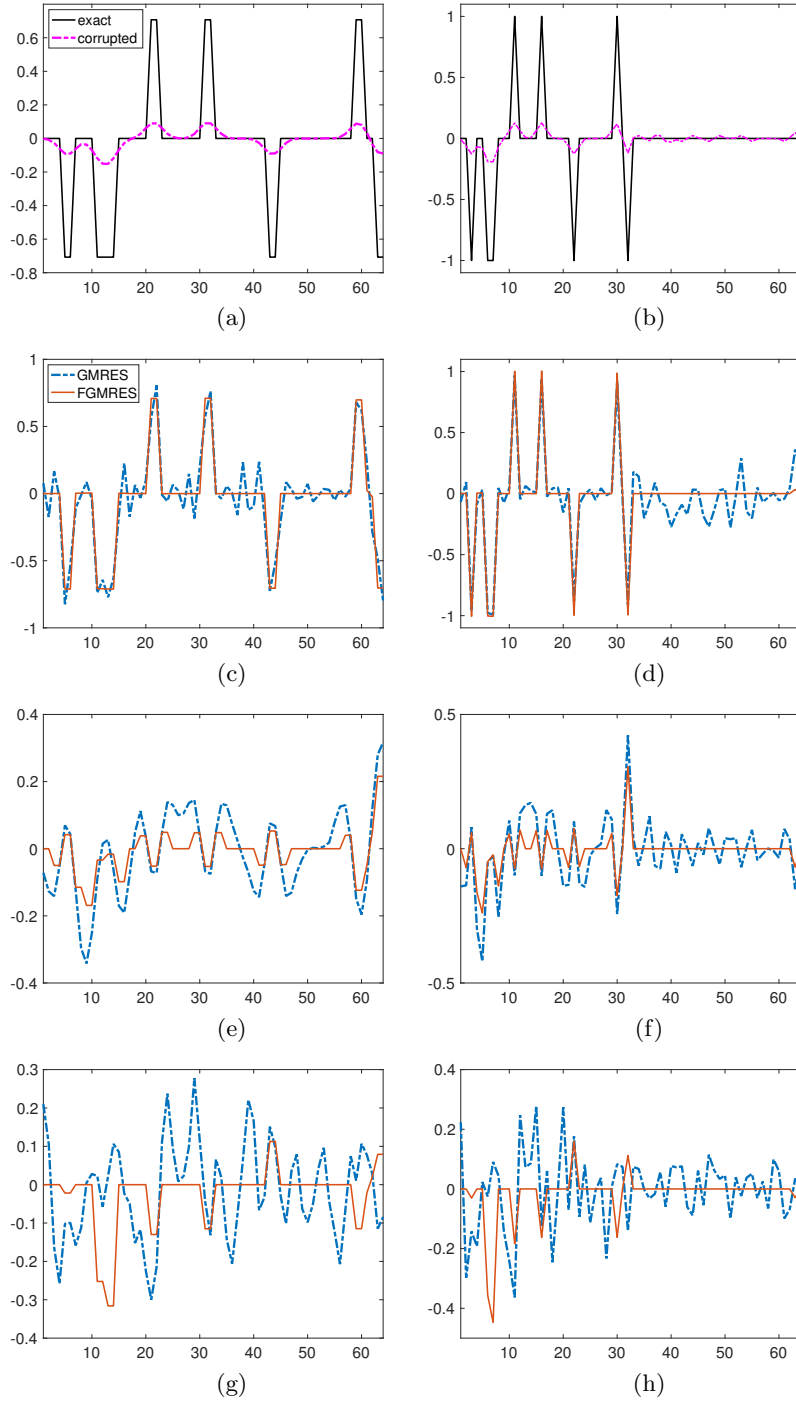


FIG. 3. 1D signal deblurring and denoising problem. The right column displays the 1D Haar wavelet coefficients of the signals displayed in the left columns. The first row shows the exact and corrupted signals. The second row shows the best reconstructions obtained by GMRES (dash-dot lines) and FGMRES (solid lines). The third and fourth row show the 2nd and 4th basis vectors computed by GMRES (dash-dot lines) and FGMRES (solid lines), respectively.

472 are performed in MATLAB 2017a and use codes available in the *Restore Tools* [27]  
 473 and *AIR Tools II* [19] software packages. MATLAB implementations of our methods,  
 474 which should be used jointly with the *IR Tools* software package [9], are available at  
 475 <https://github.com/silviagazzola>.

476 *Experiment 1.* In this experiment, we consider an image deblurring example from  
 477 atmospheric imaging, with the true image, the point spread function (PSF), and the  
 478 observed blurred image provided in Figure 4. For this problem, Gaussian white noise  
 479 is added to the blurred image, such that the noise level is  $5 \cdot 10^{-2}$ .

480 For the reconstructions, we assume reflexive boundary conditions and solve the  
 481  $\ell_1$ -regularized problem with  $\Psi = \mathbf{I}$ , which is appropriate because the desired image is  
 482 quite sparse (approximately 50% of its pixels are numerically zero). First we provide  
 483 a comparison of various Golub–Kahan–based methods. In Figure 5, we provide rela-  
 484 tive error norms per iteration for the flexible methods described in Section 3, namely  
 485 FLSQR, FLSQR-I and FLSQR-R with automatic regularization parameter selection  
 486 using the “secant update” discrepancy principle (with safety factor  $\eta = 1.01$  in (21)).  
 487 In all experiments with the discrepancy principle, we use the true noise level but  
 488 remark that estimates could be used [39]. Relative reconstruction error norms for  
 489 LSQR are provided for comparison. Similarly to the observations made in Section 3,  
 490 the flexible methods exhibit faster convergence to more accurate solutions than the  
 491 standard LSQR approach. Furthermore, we see that the flexible hybrid methods are  
 492 able to stabilize the semiconvergent behavior by selecting an appropriate regulariza-



FIG. 4. *Experiment 1: Image deblurring example.* Here we show the true image, the point spread function (PSF), and the observed blurred and noisy image. The size of the images is  $256 \times 256$  pixels.

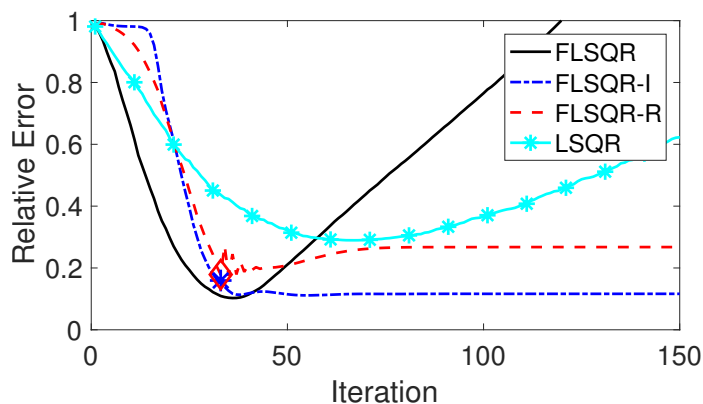


FIG. 5. *Experiment 1: Comparison of relative reconstruction error norms.* The regularization parameter  $\lambda$  is selected automatically using the “secant update method” (discrepancy principle) for ‘FLSQR-I’ and ‘FLSQR-R’;  $\lambda = 0$  is set for ‘FLSQR’ and ‘LSQR’. Automatically determined stopping iterations for the hybrid approaches are denoted by the diamond and star.



493 tion parameter and stopping criterion (e.g., based on the “secant update” strategy or  
 494 discrepancy principle).

495 In Figure 6, we provide the basis vectors (displayed as images) for the FLSQR-R  
 496 and the LSQR solution subspaces, for  $k = 10, 20, 100$ . Note that basis vectors for  
 497 FLSQR-R correspond to the FGK vectors, while the LSQR ones correspond to the  
 498 standard GKB vectors. It is evident that the basis images for the flexible method  
 499 can better capture the flat regions of the image. Also, for large  $k$ , the FLSQR-R  
 500 basis image is less affected by the noise amplification that is present in the LSQR  
 501 basis image. Thus, we expect that, by constructing a better solution basis (i.e., one  
 502 that is less affected by noise and that captures sparsity properties of the image), the  
 503 flexible methods can be successful for sparse image reconstruction. This behavior can  
 504 be experimentally observed also at higher noise levels.

505 Next, we investigate some parameter choice methods. In Figure 7, we provide relative  
 506 reconstruction error norms for FLSQR-R and ‘FLSQR-R dp’. Both methods use  
 507 the discrepancy principle to obtain the regularization parameter, which requires prior  
 508 knowledge of the noise level. More precisely, FLSQR-R utilizes the “secant update”  
 509 parameter choice method described in [10], and ‘FLSQR-R dp’ enforces the discrep-  
 510 anomaly principle to be satisfied at each iteration. Relative error norms for ‘FLSQR-R  
 511 opt’ correspond to selecting the regularization parameter at each iteration that min-  
 512 imizes the error norm of the current iterate minus the true solution. It is worth  
 513 noting that, since the basis vectors are generated with respect to the current solution  
 514 (because of flexibility), this approach does not necessarily produce the best overall  
 515 regularization parameter for the problem.

516 Finally, we compare the FLSQR-R method to other methods for solving the  $\ell_1$ -  
 517 regularized problem. In Figure 8, we provide relative reconstruction error norms for  
 518 GAT [10], PIRN, FISTA [2], and SpARSA [43]. Since the regularization parameter  
 519 for PIRN, FISTA, and SpARSA must be selected prior to execution, we use the reg-  
 520 ularization parameter that is selected by FLSQR-R when the stopping criterion is  
 521 satisfied (for this problem,  $\lambda = 1.1 \cdot 10^{-5}$ ). We note that FISTA, SpARSA, and PIRN  
 522 compute reconstructions with similar or slightly better accuracy than FLSQR-R, but  
 523 the two main advantages of the hybrid approaches are that the regularization param-

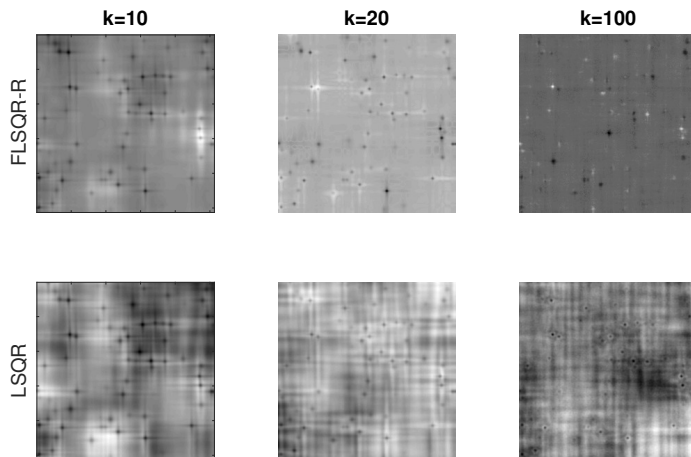


FIG. 6. Experiment 1: Basis images for ‘FLSQR-R’ and ‘LSQR’ for  $k = 10, 20, 100$ . These are solution vectors (i.e.,  $\mathbf{z}_k$  for ‘FLSQR-R’) that have been reshaped into images.

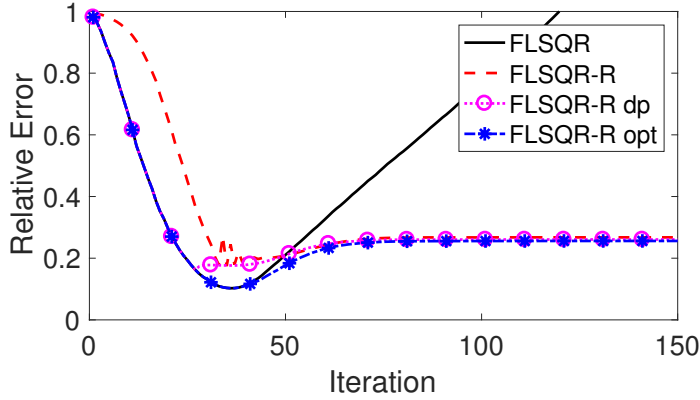


FIG. 7. *Experiment 1: Relative reconstruction error norms for different parameter choice methods. ‘FLSQR-R’ and ‘FLSQR-R dp’ use the “secant update” and the classical discrepancy principle, respectively, and thus require an estimate of the noise level. ‘FLSQR-R opt’ corresponds to selecting the optimal regularization parameter at each iteration, which is not necessarily the overall best parameter because of flexibility.*

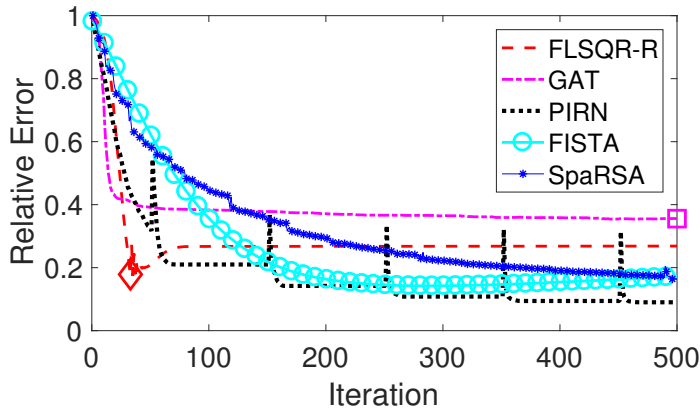


FIG. 8. *Experiment 1: Relative reconstruction error norms are provided to compare the FGK methods to some existing methods. It is important to note that the ‘PIRN’, ‘FISTA’, and ‘SpaRSA’ regularization parameter is selected using our ‘FLSQR-R’ approach.*

524 eter can be selected automatically, and the reconstruction can be obtained in fewer  
 525 iterations. The main cost per iteration for all of these methods is one matrix-vector  
 526 multiplication with  $\mathbf{A}$  and one with  $\mathbf{A}^\top$ .

527 *Experiment 2.* In this experiment, we investigate the transformed  $\ell_1$ -regularized  
 528 problem for an image deblurring example. For this problem, we use the cameraman  
 529 image shown in Figure 9, where out of focus blur (i.e., associated to a circular PSF  
 530 of radius 4 pixels) and Gaussian white noise with noise level 0.01 are considered.  
 531 Although a wide range of transformations  $\Psi$  can be employed, for simplicity we use  
 532 a 2D Haar wavelet decomposition with 3 levels. For this example, the image itself is  
 533 not sparse (only 27 pixels are numerically zero). However, slightly more than 10% of  
 534 the pixels of the transformed true image (also provided in Figure 9) are numerically  
 535 zero, and thus it is appropriate to consider the transformed  $\ell_1$ -regularized problem.

536 First we investigate the Golub–Kahan-based methods. In Figure 10, we provide  
 537 the relative reconstruction error norms for FLSQR, FLSQR-I, and FLSQR-R, where

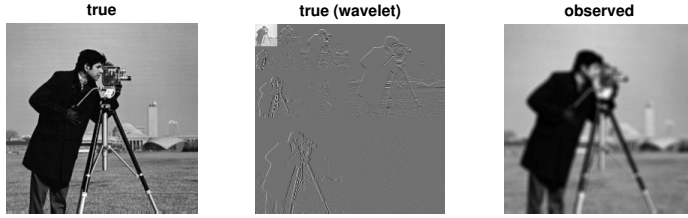


FIG. 9. Experiment 2: Image deblurring example. Here we show the true image, the wavelet coefficients of the true image, and the observed image.

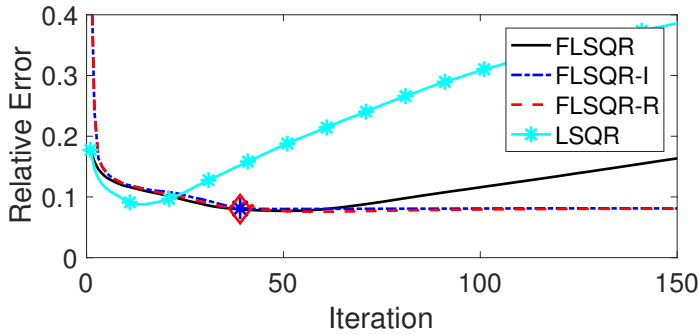


FIG. 10. Experiment 2: Relative reconstruction error norms for Golub–Kahan-based approaches. The regularization parameter  $\lambda$  is selected automatically using the discrepancy principle for ‘FLSQR-I’ and ‘FLSQR-R’;  $\lambda = 0$  is set for ‘FLSQR’ and ‘LSQR’.

538 LSQR on the original problem is provided for comparison. Although the flexible  
 539 methods take a few more iterations, they provide slightly smaller relative reconstruc-  
 540 tion errors compared to the standard solvers and the reconstructions are improved,  
 541 as evident in the displayed images. Sub-images of the best reconstructions computed  
 542 by Golub–Kahan-based methods are provided in Figure 11, along with the absolute  
 543 error sub-images  $|\mathbf{x}_k - \mathbf{x}_{\text{true}}|$ , for some values of  $k$ . The smallest relative error norm  
 544 and the iteration number (preceded by #) are reported in brackets. We observe that  
 545 although the relative error norms are comparable, the flexible methods better capture  
 546 the flat regions of the image.

547 Next we compare FLSQR-R to the GAT method applied to the transformed  
 548 problem, as well as to FISTA on the transformed problem. Here, the automatically  
 549 computed regularization parameter (i.e., the one selected by FLSQR-R upon fulfill-  
 550 ment of the discrepancy principle) is  $7.46 \cdot 10^{-5}$ , but it seems too small for FISTA.  
 551 Thus, we also provide in ‘FISTA opt’ the results for FISTA with the optimal regu-  
 552 larization parameter 0.1, which is determined by searching over 10 logarithmically  
 553 equispaced values between  $10^{-3}$  and 1, and selecting the one delivering the smallest  
 554 final relative reconstruction error norm. We observe that for a good choice of the regu-  
 555 larization parameter, FISTA reconstructions are similar to ours; however, for poor  
 556 choices of the regularization parameter, FISTA reconstructions are either too blocky  
 557 or contaminated with noise. The behavior of GAT is due a poor automatically chosen  
 558 regularization parameter.

559 Experiment 3. We consider a sparse X-ray tomographic reconstruction example  
 560 with undersampled data. The goal of this experiment is to assess the performance  
 561 of the new solvers based on the FGK decomposition for solving the transformed  $\ell_1$ -

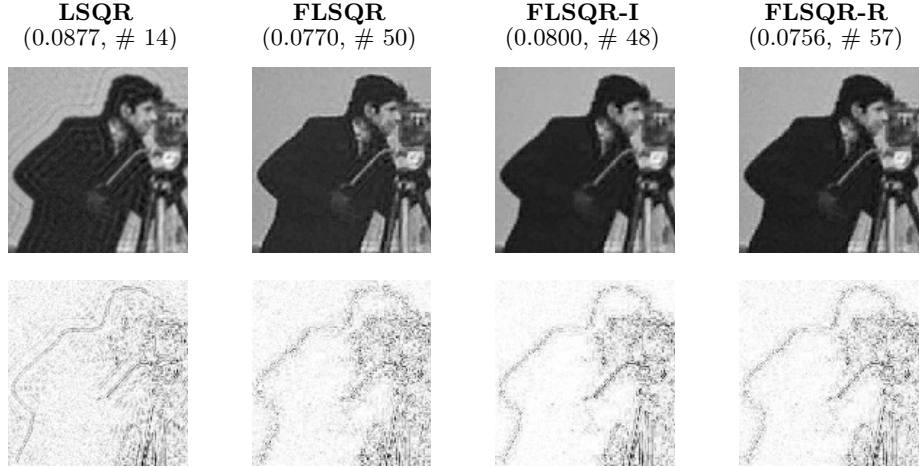


FIG. 11. *Experiment 2: Reconstructed sub-images corresponding to the smallest relative reconstruction error norm for Gobub–Kahan-based methods, along with absolute error sub-images  $|\mathbf{x}_k - \mathbf{x}_{\text{true}}|$  in inverted colormap (where white corresponds to small absolute error component). Relative reconstruction error norms and corresponding iteration numbers are reported in the titles.*

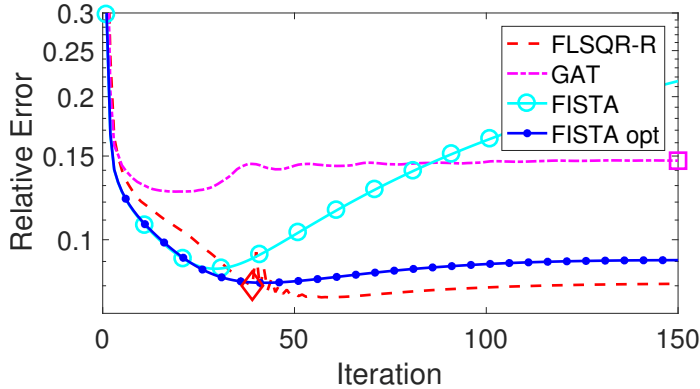


FIG. 12. *Experiment 2: Relative reconstruction error norms are provided to compare the FGK methods to some existing methods. ‘FISTA’ uses the regularization parameter selected by ‘FLSQR-R’, and ‘FISTA opt’ uses a regularization parameter that was found empirically using the true image.*

562 regularized problem (2), where  $\mathbf{A}$  is underdetermined and  $\Psi$  represents a 2D Haar  
 563 wavelet transform with 4 levels. In [21] it is empirically shown that the compressive  
 564 sensing theory applies when performing standard structured undersampling patterns  
 565 and when solving either the  $\ell_1$  or the total variation regularized problems. The test  
 566 problem considered here takes a vectorization of the well-known Shepp-Logan phan-  
 567 tom as the exact solution  $\mathbf{x}_{\text{true}}$ ; only roughly 40% of the pixels of the transformed  
 568 exact solution  $\Psi\mathbf{x}_{\text{true}}$  are numerically nonzero. A fairly underdetermined sparse ma-  
 569 trix  $\mathbf{A}$  of size  $32580 \times 65536$  (i.e., roughly 50% undersampling) is generated using  
 570 the `parallel_tomo` function from *AIR Tools II* [19], which models a 2D equidistant  
 571 parallel-beam scanning geometry, with the following parameters:

572  $N = 256$ ,  $\text{theta} = 0:2:179$ ,  $p = \text{round}(\text{sqrt}(2)*N)$ ,  $d = \text{sqrt}(2)*N$ .

573 Here  $N^2$  is the number of pixels of the phantom,  $p$  is the number of pixels of the  
 574 detector, the source-detector pair is rotated at angles of projection  $\theta$ , and  $d$  is  
 575 the distance between the first and the last ray. Note that, with such undersampling  
 576 and sparsity, and according to [21], recovery should be experimentally guaranteed.  
 577 Gaussian white noise of level  $10^{-2}$  is added to the exact data.

578 Figure 13 displays the history of the relative error norms associated with different  
 579 purely iterative regularization methods (i.e., with  $\lambda = 0$  in (23)): since we are dealing  
 580 with a rectangular matrix, only LSQR and LSMR together with their flexible versions  
 581 are considered. We can clearly see the benefits of introducing flexibility into the  
 582 solution subspaces: indeed, a greater accuracy is achieved by the flexible methods  
 583 (with a computational cost comparable to the standard solvers), together with a less  
 584 pronounced semiconvergence (this is particularly true for FLSMR, in accordance to  
 585 the observations in [5]). The only potential drawback is the doubling of the storage  
 586 requirements for FGK compared to GKB, but this is not a serious concern if the  
 587 required number of iterations  $k$  is relatively small (as it is for all of the presented test  
 588 problems).

589 Figure 14 displays the history of the relative error norms when the ‘FLSQR-I dp’  
 590 method is employed (with the regularization parameter chosen at each iteration by

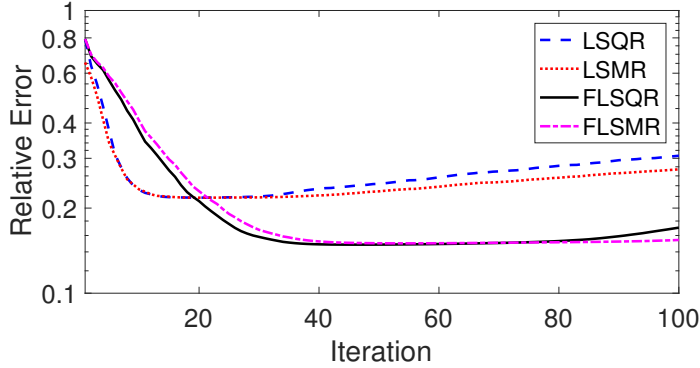


FIG. 13. Experiment 3: History of the relative error norms, considering purely iterative Golub–Kahan-based methods.

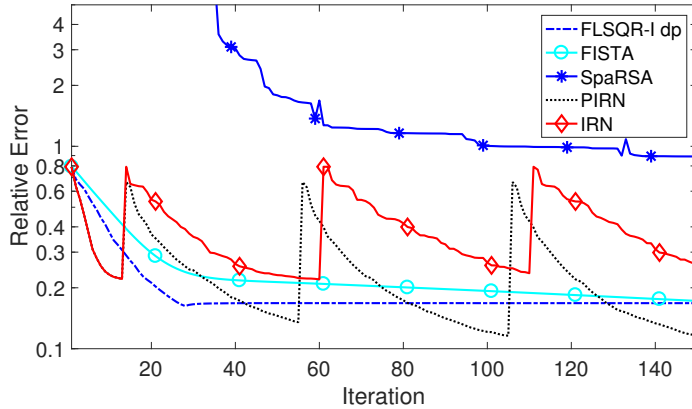


FIG. 14. Experiment 3: History of the relative error norms, comparing the ‘FLSQR-I’ method to ‘FISTA’, ‘SpaRSA’, ‘IRN’, and ‘PIRN’.

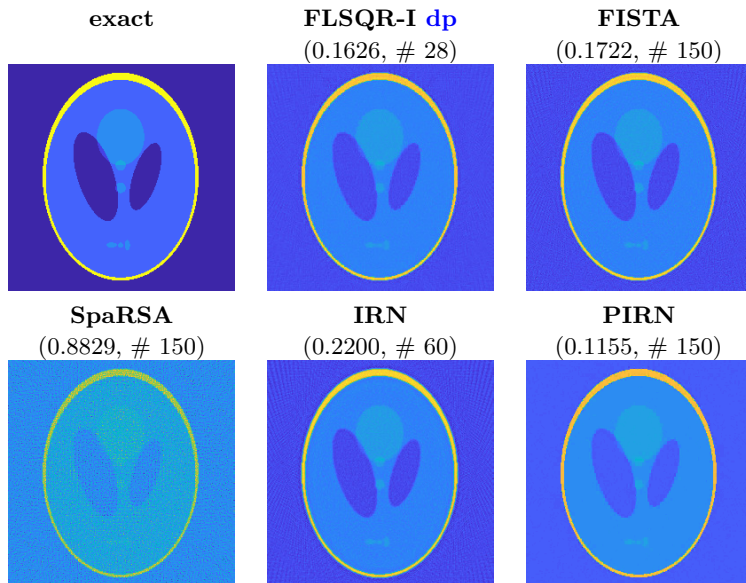


FIG. 15. *Experiment 3: Reconstructed sub-images of best quality for various solvers. Smallest attained relative reconstruction error norms (up to 150 iterations) and corresponding iteration numbers (preceded by #) are reported.*

591 the discrepancy principle), and compares it to other solvers for (23). In particular, we  
 592 compare with FISTA, SpaRSA, IRN, and PIRN. As already remarked, all of these well-  
 593 established solvers require the regularization parameter  $\lambda$  to be set at the beginning  
 594 of the iterative process: for this experiment we choose  $\lambda = 4.2 \cdot 10^{-5}$ , which is the  
 595 value computed by the classical discrepancy principle at the end of the ‘FLSQR-I dp’  
 596 iterations (when also some stabilization occurred in the iteration-dependent values  
 597 of the regularization parameter). We can clearly see that SpaRSA does not perform  
 598 well for this problem, and a more accurate tuning of the regularization parameter  
 599 may improve its reconstruction. FISTA requires more iterations than ‘FLSQR-I dp’  
 600 to compute reconstructions of similar quality. Both SpaRSA and FISTA depend  
 601 heavily on a good choice of the regularization parameter. Of the considered methods,  
 602 the PIRN method results in the smallest relative reconstruction error norms, but it  
 603 requires more iterations than ‘FLSQR-I dp’ to reach an optimal accuracy. PIRN also  
 604 outperforms IRN, which is not so effective because of the small  $\lambda$  considered in this  
 605 framework. The quality of the reconstruction does not significantly improve when  
 606 additional PIRN or IRN iterations are performed. We do not show the behavior of  
 607 the FLSQR-R, FLSMR-I, and FLSMR-R hybrid methods as they are very similar to  
 608 the FLSQR-I method for this problem.

609 Figure 15 shows the best reconstructions computed by each method considered  
 610 in Figure 14. The best relative error and the iteration number (preceded by #) are  
 611 reported in brackets. Again, we remark that the computational cost for each iteration  
 612 of these methods is dominated by a matrix-vector product with  $\mathbf{A}$  and one with  $\mathbf{A}^\top$ .

613 **6. Conclusions and future work.** In this paper, we describe flexible hy-  
 614 brid iterative methods for computing approximate solutions to the (transformed)  
 615  $\ell_p$ -regularized problem, for  $p \geq 1$ . To handle general (non-square)  $\ell_p$ -regularized  
 616 least-squares problems, we introduce a flexible Golub–Kahan approach and exploit



617 it within a Krylov–Tikhonov hybrid framework. Theoretical results show that the  
 618 iterates correspond to solutions of a full-dimensional Tikhonov problem that has been  
 619 projected onto flexible Krylov subspaces of increasing dimensions. We describe var-  
 620 ious extensions for effectively computing solutions that are sparse with respect to  
 621 some invertible transformation. Our proposed methods are *efficient* in that they can  
 622 access  $\mathbf{A}$  and  $\mathbf{A}^\top$  as function evaluations and they avoid inner-outer schemes, and  
 623 *automatic* in that parameters such as regularization parameters and stopping itera-  
 624 tions can be naturally selected within a hybrid framework. Numerical results validate  
 625 these observations.

626 Future work includes extensions to problems where  $\Psi$  is not invertible, and also  
 627 to nonlinear regularization functionals (e.g., total variation) and nonconvex problems.  
 628 Developing theoretical convergence results for flexible methods requires additional in-  
 629 vestigation and would also apply to other solvers based on flexible preconditioning,  
 630 e.g., [10, 12]. Furthermore, by incorporating multi-level decompositions, these flexi-  
 631 ble hybrid methods can be exploited in a multi-parameter regularization framework,  
 632 where a different sparsity regularization parameter is incorporated for each level.

633 **Acknowledgments.** The authors are grateful to the anonymous referees for  
 634 their detailed reading of the manuscript and for providing insightful remarks that  
 635 helped to improve our paper. Also, the authors would like to thank the Isaac Newton  
 636 Institute for Mathematical Sciences for support and hospitality during the programme  
 637 “Variational methods and effective algorithms for imaging and vision” when work on  
 638 this paper was undertaken.

639

## REFERENCES

- 640 [1] S. ARRIDGE, M. BETCKE, AND L. HARHANEN, *Iterated preconditioned LSQR method for inverse*  
 641 *problems on unstructured grids*, Inverse Problems, 30 (2014), p. 075009, [https://doi.org/](https://doi.org/10.1088/0266-5611/30/7/075009)  
 642 [10.1088/0266-5611/30/7/075009](https://doi.org/10.1088/0266-5611/30/7/075009).
- 643 [2] A. BECK AND M. TEOULLE, *A fast iterative shrinkage-thresholding algorithm for linear inverse*  
 644 *problems*, SIAM J. Imaging Sci., 2 (2009), pp. 183–202, <https://doi.org/10.1137/080716542>.
- 645 [3] M. BELGE, M. E. KILMER, AND E. L. MILLER, *Wavelet domain image restoration with adaptive*  
 646 *edge-preserving regularization*, IEEE Trans. Image Process., 9 (2000), pp. 597–608, [https:](https://doi.org/10.1109/83.841937)  
 647 [//doi.org/10.1109/83.841937](https://doi.org/10.1109/83.841937).
- 648 [4] Å. BJÖRCK, *Numerical Methods for Least Squares Problems*, SIAM, Philadelphia, PA, 1996,  
 649 <https://doi.org/10.1137/1.9781611971484>.
- 650 [5] J. CHUNG AND K. PALMER, *A hybrid LSMR algorithm for large-scale Tikhonov regularization*,  
 651 SIAM J. Sci. Comput., 37 (2015), pp. S562–S580, <https://doi.org/10.1137/140975024>.
- 652 [6] I. DAUBECHIES, M. DEFRISE, AND C. DE MOL, *An iterative thresholding algorithm for lin-*  
 653 *ear inverse problems with a sparsity constraint*, Communications on Pure and Applied  
 654 Mathematics, 57 (2004), pp. 1413–1457, <https://doi.org/10.1137/140975024>.
- 655 [7] M. I. ESPANOL AND M. E. KILMER, *A wavelet-based multilevel approach for blind deconvolution*  
 656 *problems*, SIAM J. Sci. Comput., 36 (2014), pp. A1432–A1450, [https://doi.org/10.1137/](https://doi.org/10.1137/130928716)  
 657 [130928716](https://doi.org/10.1137/130928716).
- 658 [8] D. C.-L. FONG AND M. SAUNDERS, *LSMR: An iterative algorithm for sparse least-squares*  
 659 *problems*, SIAM J. Sci. Comput., 33 (2011), pp. 2950–2971, [https://doi.org/10.1137/](https://doi.org/10.1137/10079687X)  
 660 [10079687X](https://doi.org/10.1137/10079687X).
- 661 [9] S. GAZZOLA, P. C. HANSEN, AND J. G. NAGY, *IR Tools: A MATLAB package of iterative*  
 662 *regularization methods and large-scale test problems*, Numer. Algorithms, (2018), [https:](https://doi.org/10.1007/s11075-018-0570-7)  
 663 [//doi.org/10.1007/s11075-018-0570-7](https://doi.org/10.1007/s11075-018-0570-7).
- 664 [10] S. GAZZOLA AND J. G. NAGY, *Generalized Arnoldi–Tikhonov method for sparse reconstruction*,  
 665 SIAM J. Sci. Comput., 36 (2014), pp. B225–B247, <https://doi.org/10.1137/130917673>.
- 666 [11] S. GAZZOLA, P. NOVATI, AND M. R. RUSSO, *On Krylov projection methods and Tikhonov*  
 667 *regularization*, Electron. Trans. Numer. Anal., 44 (2015), pp. 83–123.
- 668 [12] S. GAZZOLA AND Y. WIAUX, *Fast nonnegative least squares through flexible Krylov subspaces*,  
 669 SIAM J. Sci. Comput., 39 (2017), pp. A655–A679, <https://doi.org/10.1137/15M1048872>.



- 670 [13] R. GIRYES, M. ELAD, AND Y. C. ELДАР, *The projected GSURE for automatic parameter tuning*  
671 *in iterative shrinkage methods*, Appl. Comput. Harmon. Anal., 30 (2011), pp. 407–422,  
672 <https://doi.org/10.1016/j.acha.2010.11.005>.
- 673 [14] T. GOLDSTEIN AND S. OSHER, *The split Bregman method for  $l_1$ -regularized problems*, SIAM J.  
674 Imaging Sci., 2 (2009), pp. 323–343, <https://doi.org/10.1137/080725891>.
- 675 [15] G. GOLUB AND W. KAHAN, *Calculating the singular values and pseudo-inverse of a matrix*,  
676 Journal of the Society for Industrial and Applied Mathematics, Series B: Numerical Anal-  
677 ysis, 2 (1965), pp. 205–224, <https://doi.org/10.1137/0702016>.
- 678 [16] I. F. GORODNITSKY AND B. D. RAO, *A new iterative weighted norm minimization algorithm and*  
679 *its applications*, in IEEE Sixth SP Workshop on Statistical Signal and Array Processing,  
680 1992, pp. 412–415, <https://doi.org/10.1109/SSAP.1992.246872>.
- 681 [17] P. C. HANSEN, *Regularization tools: A matlab package for analysis and solution of dis-*  
682 *crete ill-posed problems*, Numer. Algorithms, (1994), pp. 1–35, <https://doi.org/10.1007/>  
683 [BF02149761](https://doi.org/10.1007/BF02149761).
- 684 [18] P. C. HANSEN, *Discrete Inverse Problems: Insight and Algorithms*, SIAM, 2010, <https://doi.org/10.1137/1.9780898718836>.
- 685 [19] P. C. HANSEN AND J. S. JORGENSEN, *AIR Tools II: Algebraic Iterative Reconstruction*  
686 *Methods, Improved Implementation*, Numer. Algorithms, (2018), [https://doi.org/10.1007/](https://doi.org/10.1007/s11075-017-0430-x)  
687 [s11075-017-0430-x](https://doi.org/10.1007/s11075-017-0430-x).
- 688 [20] G. HUANG, A. LANZA, S. MORIGI, L. REICHEL, AND F. SGALLARI, *Majorization–minimization*  
689 *generalized Krylov subspace methods for  $\ell_p - \ell_q$  optimization applied to image restoration*,  
690 BIT, 57 (2017), pp. 351–378, <https://doi.org/10.1007/s10543-016-0643-8>.
- 691 [21] J. S. JORGENSEN AND E. Y. SIDKY, *How little data is enough? Phase-diagram analysis of*  
692 *sparsity-regularized X-ray computed tomography*, Phil. Trans. R. Soc. A, 373: 20140387  
693 (2015), <https://doi.org/10.1098/rsta.2014.0387>.
- 694 [22] M. E. KILMER AND D. P. O’LEARY, *Choosing regularization parameters in iterative methods*  
695 *for ill-posed problems*, SIAM J. Matrix Anal. Appl., 22 (2001), pp. 1204–1221, <https://doi.org/10.1137/S0895479899345960>.
- 696 [23] E. KLANN, R. RAMLAU, AND L. REICHEL, *Wavelet-based multilevel methods for linear ill-posed*  
697 *problems*, BIT, 51 (2011), pp. 669–694, <https://doi.org/10.1007/s10543-011-0320-x>.
- 698 [24] A. LANZA, S. MORIGI, L. REICHEL, AND F. SGALLARI, *A generalized Krylov subspace method*  
699 *for  $\ell_p - \ell_q$  minimization*, SIAM J. Sci. Comput., 37 (2015), pp. S30–S50, <https://doi.org/10.1137/140967982>.
- 700 [25] A. LANZA, S. MORIGI, I. SELESNICK, AND F. SGALLARI, *Nonconvex nonsmooth optimization via*  
701 *convex - nonconvex majorization - minimization*, Numer. Math., 136 (2017), pp. 343–381,  
702 <https://doi.org/10.1007/s00211-016-0842-x>.
- 703 [26] K. MORIKUNI AND K. HAYAMI, *Convergence of inner-iteration GMRES methods for rank-*  
704 *deficient least squares problems*, SIAM J. Matrix Anal. Appl., 36 (2015), pp. 225–250,  
705 <https://doi.org/10.1137/130946009>.
- 706 [27] J. G. NAGY, K. PALMER, AND L. PERRONE, *Iterative methods for image deblurring: a MATLAB*  
707 *object-oriented approach*, Numer. Algorithms, 36 (2004), pp. 73–93, [https://doi.org/10.](https://doi.org/10.1023/B:NUMA.0000027762.08431.64)  
708 [1023/B:NUMA.0000027762.08431.64](https://doi.org/10.1023/B:NUMA.0000027762.08431.64).
- 709 [28] Y. NOTAY, *Flexible conjugate gradients*, SIAM J. Sci. Comput., 22 (2000), pp. 1444–1460,  
710 <https://doi.org/10.1137/S1064827599362314>.
- 711 [29] D. P. O’LEARY AND J. A. SIMMONS, *A bidiagonalization-regularization procedure for large scale*  
712 *discretizations of ill-posed problems*, SIAM J. Sci. and Stat. Comput., 2 (1981), pp. 474–  
713 489, <https://doi.org/10.1137/0902037>.
- 714 [30] C. C. PAIGE AND M. A. SAUNDERS, *Algorithm 583: LSQR: Sparse linear equations and least*  
715 *squares problems*, ACM Trans. Math. Software, 8 (1982), pp. 195–209, [https://doi.org/10.](https://doi.org/10.1145/355993.356000)  
716 [1145/355993.356000](https://doi.org/10.1145/355993.356000).
- 717 [31] C. C. PAIGE AND M. A. SAUNDERS, *LSQR: An algorithm for sparse linear equations and sparse*  
718 *least squares*, ACM Trans. Math. Software, 8 (1982), pp. 43–71, [https://doi.org/10.1145/](https://doi.org/10.1145/355984.355989)  
719 [355984.355989](https://doi.org/10.1145/355984.355989).
- 720 [32] R. A. RENAUT, S. VATANKHAH, AND V. E. ARDESTANI, *Hybrid and iteratively reweighted reg-*  
721 *ularization by unbiased predictive risk and weighted GCV for projected systems*, SIAM J.  
722 Sci. Comput., 39 (2017), pp. B221–B243, <https://doi.org/10.1137/15M1037925>.
- 723 [33] P. RODRIGUEZ AND B. WOHLBERG, *An efficient algorithm for sparse representations with*  
724  *$\ell^p$  data fidelity term*, in Proceedings of 4th IEEE Andean Technical Conference (AN-  
725 DESCON), 2008.
- 726 [34] Y. SAAD, *On the rates of convergence of the Lanczos and the block-Lanczos methods*, SIAM J.  
727 Numer. Anal., 17 (1980), pp. 687–706, <https://doi.org/10.1137/0717059>.
- 728 [35] Y. SAAD, *A flexible inner-outer preconditioned GMRES algorithm*, SIAM J. Sci. Comput., 14

- 732 (1993), pp. 461–469, <https://doi.org/10.1137/0914028>.
- 733 [36] A. K. SAIBABA, T. BAKHOS, AND P. K. KITANIDIS, *A flexible Krylov solver for shifted systems*  
734 *with application to oscillatory hydraulic tomography*, SIAM J. Sci. Comput., 35 (2013),  
735 pp. A3001–A3023, <https://doi.org/10.1137/120902690>.
- 736 [37] V. SIMONCINI AND D. B. SZYLD, *Flexible inner-outer Krylov subspace methods*, SIAM J. Numer.  
737 Anal., 40 (2002), pp. 2219–2239, <https://doi.org/10.1137/s0036142902401074>.
- 738 [38] V. SIMONCINI AND D. B. SZYLD, *Recent computational developments in Krylov subspace*  
739 *methods for linear systems*, Numer. Linear Algebra Appl., 14 (2007), pp. 1–59, <https://doi.org/10.1002/nla.499>.
- 740 [39] L. TENORIO, *An Introduction to Data Analysis and Uncertainty Quantification for Inverse*  
741 *Problems*, SIAM, Philadelphia, 2017, <https://doi.org/10.1137/1.9781611974928>.
- 742 [40] J. A. TROPP AND S. J. WRIGHT, *Computational methods for sparse solution of linear inverse*  
743 *problems*, Proceedings of the IEEE, 98 (2010), pp. 948–958, [https://doi.org/10.21236/](https://doi.org/10.21236/ada633835)  
744 [ada633835](https://doi.org/10.21236/ada633835).
- 745 [41] J. VAN DEN ESHOF AND G. L. SLEJPEN, *Inexact Krylov subspace methods for linear sys-*  
746 *tems*, SIAM J. Matrix Anal. Appl., 26 (2004), pp. 125–153, [https://doi.org/10.1137/](https://doi.org/10.1137/s0895479802403459)  
747 [s0895479802403459](https://doi.org/10.1137/s0895479802403459).
- 748 [42] S. VATANKHAH, R. A. RENAUT, AND V. E. ARDESTANI, *3-D projected L1 inversion of grav-*  
749 *ity data using truncated unbiased predictive risk estimator for regularization param-*  
750 *eter estimation*, Geophysical Journal International, 210 (2017), pp. 1872–1887, <https://doi.org/10.1093/gji/ggx274>.
- 751 [43] S. J. WRIGHT, R. D. NOWAK, AND M. A. FIGUEIREDO, *Sparse reconstruction by separable*  
752 *approximation*, IEEE Trans. Signal Process., 57 (2009), pp. 2479–2493, [https://doi.org/](https://doi.org/10.1109/icassp.2008.4518374)  
753 [10.1109/icassp.2008.4518374](https://doi.org/10.1109/icassp.2008.4518374).
- 754
- 755